J Mol Model (2008) 14:225–235
DOI 10.1007/s00894-007-0265-9

ORIGINAL PAPER

Molecular dynamics simulation of hydrated Nafion with a reactive force field for water

Detlef W. M. Hofmann · Liudmila Kuleshova · Bruno D'Aguanno

Received: 15 August 2007 / Accepted: 13 December 2007 / Published online: 18 January 2008

Abstract We apply a newly parameterized central force field to highlight the problem of proton transport in fuel cell membranes and show that central force fields are potential candidates to describe chemical reactions on a classical level. After a short sketch of the parameterization of the force field, we validate the obtained force field for several properties of water. The experimental and simulated radial distribution functions are reproduced very accurately as a consequence of the applied parameterization procedure. Further properties, geometry, coordination, diffusion coefficient and density, are simulated adequately for our purposes. Afterwards we use the new force field for the molecular dynamics simulation of a swollen polyelectrolyte membrane similar to the widespread Nafion 117. We investigate the equilibrated structures, proton transfer, lifetimes of hydronium ions, the diffusion coefficients, and the conductivity in dependence of water content. In a short movie we demonstrate the ability of the obtained force field to describe the bond breaking/formation, and conclude that this force field can be considered as a kind of a reactive force field. The investigations of the lifetimes of hydronium ions give us the information about the kinetics of the proton transfer in a membrane with low water content. We found the evidence for the second order reaction. Finally, we demonstrate that the model is simple enough to handle the large systems sufficient to calculate the conductivity from molecular dynamics simulations. The detailed analysis of the conductivity reveals the importance of the collective moving of hydronium ions in membrane, which might give an interesting encouragement for further development of membranes. Figure: The structure of water in one pore of the highly hydrated Nafion membranes.

Keywords Molecular dynamics · Nafion · Radial distribution function · Reactive force field · Water

Electronic supplementary material The online version of this article (doi:10.1007/s00894-007-0265-9) contains supplementary material, which is available to authorized users.

D. W. M. Hofmann (✉) · L. Kuleshova · B. D'Aguanno
CRS4, Parco Scientifico e Tecnologico, Sardegna Recerca,
Edificio 1,
09010 Pula, Italy
e-mail: hofmann@crs4.it

Introduction

The polyelectrolyte membranes are aimed to separate the anode and cathode gases and/or liquids, and to mediate the electrochemical reactions occurring at the electrodes. The transport of charged species in the membrane is required to be fast and highly selective. For development of improved or new proton conducting membranes it is extremely important to understand the underlying elementary processes in these membranes. A recent overview of the present state on the conducting mechanism and the proton conductivity in membranes can be found at Kreuer et al. [1].

The modeling of polyelectrolyte membranes (for example Nafion), on different theoretical levels, has provided many insights into membrane structure and function, included morphology, structure and properties of absorbed water, proton transport, role of a side chain, dissociation of the SO_3H-group and so on. For a successful modeling the challenges are the importance of the Grotthuss mechanism for the conductivity and the simulation of water itself. Grotthuss mechanism of proton transfer is caused by the formation and dissociation H-O covalent bonds; therefore it can be straight forward simulated by quantum molecular dynamics, which is restricted to a few particles. On the

level of semiclassical molecular dynamics the proton transfer has been studied very detailed in small water clusters [2].

More extended systems including the membranes require some simplification in the method to achieve lower CPU-times. Such simplification has been achieved by the valence bond theory. On this level the problem has been addressed by various groups. The proton transport including the Grotthuss mechanism of diffusion was investigated with the empirical valence bond EVB [3, 4] or EVB2-type [5] model. Such kind of simulations on representative Nafion models have been carried out, for example, by Spohr [6] and Petersen [7].

An alternative possibility to take into account Grotthuss transport in classical MD can be given by reactive force fields (RFF) developed recently by several groups [8, 9]. The parameters for the RFF have been obtained from quantum mechanics. These force fields close the gap between quantum mechanics and traditional force field simulations and open new possibilities to treat in computer simulations the large, complicate, and reactive systems.

The second problem is the correct simulation of the water structure itself. A lot of classical and quantum mechanical simulations fail to reproduce the experimental radial distribution functions (RDF) [10] and X-ray scattering data [11]. However, the correct structure and, as a consequence, the scattering data are the main target of molecular modeling. Therefore some efforts have been made to use structural data for the calibration of force fields [12, 13].

The connected mathematical task of these efforts is well known in science as an inverse problem and can be solved by different recursive fitting procedures. Here we present an effective force field obtained by recursive fitting to the radial distribution functions of water at different temperatures and pressures. We show that the obtained model reproduces correctly the geometrical properties of water and some thermodynamical properties of interest, self-diffusion coefficients and density. It demonstrates as well the general possibility to obtain bond breaking/formation within a fully classical approach. The new reactive force field is applied finally to simulate a Nafion membrane at different hydration levels. The results of the simulations are analyzed for the kinetics of the protons, the diffusion coefficients, and the conductivity.

Reactive force field of water

Method

To construct our reactive force field for water we choose the central force model. The interesting feature of the central force field for water [14–16] is its intrinsic property to allow bond breaking/formation. We reparameterized the central force field model. The parameterization was done by recursive fitting to the radial distribution functions obtained at different temperatures and pressures. We used the data sets available from the ISIS Disordered Materials Group Neutron Database (www.isis.rl.ac.uk/""disordered/""database/""DBMain.htm) [12]. For the recursive fitting we used an empirical potential structure refinement [17, 18]. This algorithm has been successfully applied to derive intermolecular interaction potentials.

In the central force model water is considered as an electrolyte. Hydrogen and oxygen atoms are the individual entities that can eventually associate to form molecules. In this model the potential energy E_{pot} is written as the sum of the pair interactions between the N atoms of a given system:

$$E_{pot} \approx E_2 = \sum_{m>n}^{N} e_{mnr} \tag{1}$$

For further simplifications to each atom n and m, an atom type is assigned and the above formula can be rewritten:

$$e_{mnr} \approx e_{type(m)type(n)r_{mn}} = \varepsilon_{ijr} \tag{2}$$

The pair potentials ε_{ijr} are split into two parts to take the electrostatic interaction into account: a short range ε^{sr} and a long range, coulomb potential $\varepsilon^{coulomb}$.

$$\varepsilon_{ijr} = \varepsilon_{ijr}^{sr} + \varepsilon_{ijr}^{coulomb} = \varepsilon_{ijr}^{sr} + \frac{q_i q_j}{4\pi\varepsilon_0 r_{ij}} \tag{3}$$

Since the experimental RDF's do not show recognizable structural features after 7Å the cutoff r_{cutoff} for deriving pair potentials ε^{sr} was taken at 7Å. Beyond 7Å the potentials ε_{ijr} were continued by long range Coulomb term $\varepsilon^{coulomb}$.

For the atomic charges in the Coulomb term one can find different values in the literature. We took the values of −0.834 e for oxygen and +0.417 e for hydrogen atoms. These values were used in a number of publications for water [19], as well as for membrane simulations [3, 20] and guarantee a correct dipole moment for water.

The short range term ε^{sr} of Eq. 3 has been determined by the empirical potential structure refinement. The procedure was modified to fit to our problem [21]. First of all the potentials were fitted over the full range of distances and therefor the potentials were not further divided into inter- and intra-molecular parts. This is in correspondence to the basic idea of central force fields. Secondly, the potentials were optimized for three different data sets at different temperature and pressure. This reduces the problem of overfitting and requires a changed expression for the cost function during the fitting procedure. Finally we added a validation of the obtained potential with the test data set to exclude an overfitting.

For the optimizing procedure we selected three experimentally determined RDFs at different temperatures and pressures: dense water ($T=268$ K and $p=27$ MPa), the data set at standard condition ($T=298$ K and $p=0.1$ MPa), and a data set at high temperature ($T=423$ K and $p=10$ MPa).

The simulated radial distribution functions g^{sim} of water were obtained from MD simulations with DL_POLY2. The initial configuration was generated by putting randomly 2000 hydrogen and 1000 oxygen atoms in a cube with 30 Å lengths. The equilibration of the system was performed in the NPT ensemble with a time step of 0.2 *fs* over 200000 time steps. Then the production run was performed in the NVT ensemble for 40 ps. From the stored trajectory the radial distribution functions g^{sim} were evaluated.

The cost function J included all three experiments. The similarity for an experimental and a simulated radial distribution function s^{RDF} can be expressed by the mean square deviation of the logarithmized values.

$$s^{RDF} = \frac{1}{r_{cutoff}} \int_0^{r_{cutoff}} \left(\frac{\ln g^{sim}}{\ln g^{\exp}} \right)^2 dr \tag{4}$$

The similarity index for a data set s^{set} at given temperature and pressure was calculated as mean of the three radial distribution functions g_{OO}, g_{OH} and g_{HH}.

$$s^{set} = \frac{s^{RDF}_{OO} + s^{RDF}_{OH} + s^{RDF}_{HH}}{3} \tag{5}$$

The total cost function J has been written as the arithmetic mean between the individual similarities of the different data sets.

$$J = \frac{s^{set}_{268,27} + s^{set}_{298,0.1} + s^{set}_{423,10}}{3} \tag{6}$$

After training the obtained potentials were validated on a test system IV ($T=298$ K and $p=210$ MPa), to be sure that we exclude an overfitting in our procedure. The overfitting is an inherent characteristic of solving inverse problems with a huge number of parameters. In such a case the data used for the fitting procedure, the training set, are reproduced perfectly. However, the parameters become arbitrary for any other data not included in the training set. For this reason it is strongly recommended in recursive fitting procedures to validate the obtained parameters for a validation set. Therefore we checked our potentials for a fourth set of radial distribution functions measured at different conditions.

In Fig. 1 we show the resulting effective potentials derived by the sketched fitting procedure. The potentials coincide qualitatively with the CFM potentials derived in former publications.

Radial distribution functions

The developed pair potential functions have been firstly verified for the RDF's. MD simulations have been performed for four water systems (for details see the Section Method). For all four systems the experimental and simulated RDFs coincide very well (see Fig. 2). The RMSD between the RDFs is below 0.03%: $s^{set}_{268,27} = 0.025$, $s^{set}_{298,0.1} = 0.025$, $s^{set}_{423,10} = 0.030$ and $s^{set}_{298,210} = 0.029$. The resulting similarity indices show good accuracy for the training data sets, as well as for the test data ($T=298$ K and $p=210$ MPa). From the presented results it follows that the developed average RFF reflects the changing in RDFs of water caused by variations of temperatures and pressures. The good agreement of simulated and experimental RDF obtained for the test data set proves that a possible overfitting is avoided in our procedure.

Structural properties

Further the new force field has been tested on the reproduction of the structure and dynamic properties of water at standard condition. A first impression of the equilibrated water structure one can get from Fig. 3. The visualized structure of water satisfies the general expectation of chemists. Mostly all hydrogen and oxygen atoms formed water molecules. A large part of the oxygen atom has a pseudo-tetrahedral coordination, two covalently bonded hydrogen atoms and two hydrogen bond bridges. The geometry of hydrogen bridges is mainly linear.

To study the structure of simulated water in more detail we split the RDF g_{OH} into the individual contributions of the five closest hydrogen atoms (Fig. 4).

The obtained distribution confirms the visual impression of Fig. 3. The majority of oxygen atoms are covalently bonded to two hydrogen atoms (red and black curves). Moreover they are coordinated by hydrogen bridges to the other two hydrogen atoms (green and blue curves). The distribution of the nearest (first) group of hydrogen atoms has an average distance of 0.90Å (black curve), the distribution of the second group of hydrogen atoms has an average distance of 1.00Å (red curve). The distributions of the hydrogen bridges, represented by the third and fourth groups of hydrogen, are more diffused than the covalent bonds. The centers of the distributions are at a distance of 1.75Å (green) and 1.95Å (blue). A similar predominant structure with a tetrahedral surrounding of water molecule was found previously by fitting experimental X-ray absorption spectra [11].

The third group of hydrogen atoms (green curve) gives an additional small maximum around 1.10Å. This peak shows the presence of a small number of oxygen atoms covalently bonded to three hydrogen atoms (hydronium

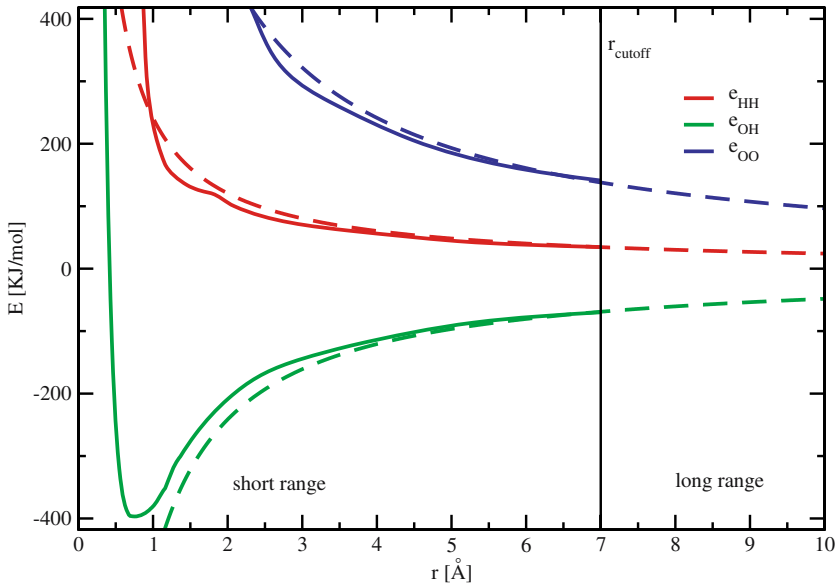

Fig. 1 Reactive water potentials. The short range potentials are in full lines. After the cutoff at 7Å the potentials are continued by the coulomb interaction (dashed lines)

ions). Similar, the low intense peak of the second group of hydrogen atoms (red curve) at 1.60Å reflects the presence of hydroxyl ions. The major amount of these ions is presented as a contact ionic pair $(H_3O^+)(OH^-)$and corresponds to the fluctuations of a hydrogen atom between two water molecules. This follows from the detailed analysis of the radial distribution functions for H_3O^+ and OH^-.

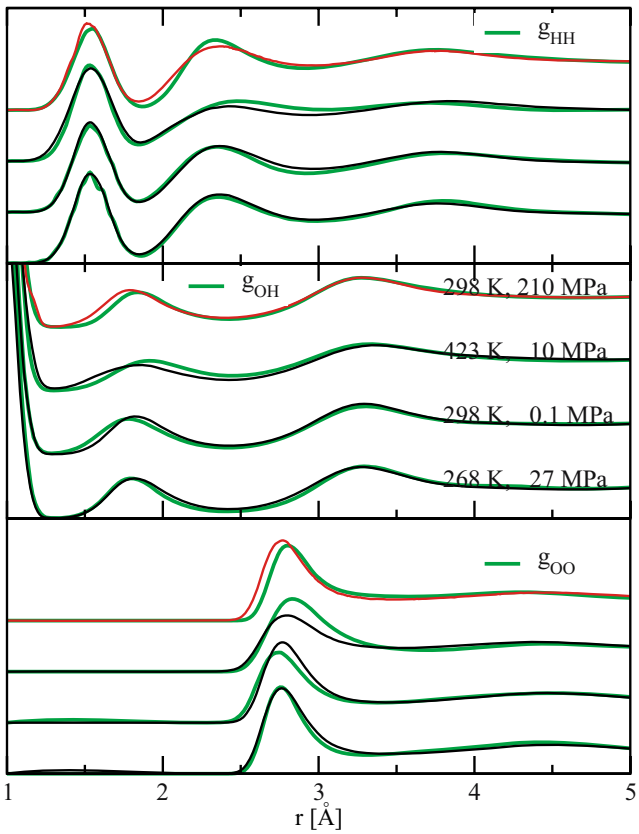

Fig. 2 Comparison between experimental (green) and simulated RDF's. The three training sets (black) and the validation set (red) match very well with the experimental RDF's

Dynamical properties

We checked also the density and dynamic properties (self-diffusion coefficients) of simulated reactive water model. The results are summarized in Table 1. The density ρ_{sim} derived by MD under NPT conditions shows in all cases good agreement with the experimental data taken from [12] and differs in the worst case by 8%, which indirectly justifies the quality of the obtained water structure.

The approximative description of the self-diffusion coefficients in water is a requirement for the qualitative investigation of conductivity in Nafion membranes. The diffusion coefficients in our model are underestimated from 30% to 40%, but the temperature dependence of the diffusion coefficients is reproduced precisely. This accuracy

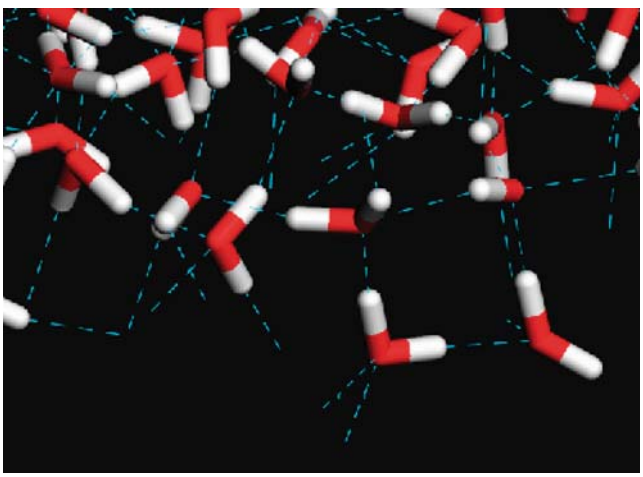

Fig. 3 Configuration of water after equilibration at standard condition

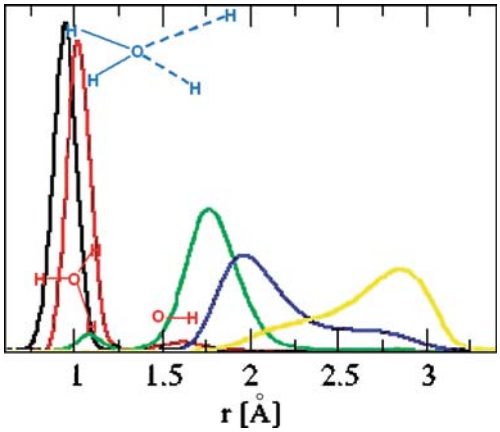

Fig. 4 The frequencies of the five closest hydrogen atoms

is adequate for the considerations made in the following chapters. The advantage of the model to allow bond-breaking/formation outweighs the accurate reproduction of diffusion coefficients of other models, e.g., [22, 23]. Compared to an extended list of simulated diffusion coefficients for 42 different water models [24] the values are reasonably reproduced. The values obtained by empirical methods vary from $1.1*10^{-9}$ m^2/s [25] to $4.3*10^{-9}$ m^2/s [26]. *Ab initio* methods reproduce the diffusion coefficient better, but still spread between $1.2*10^{-9}$ m^2/s [27] and $2.8*10^{-9}$ m^2/s [28].

MD simulations of hydrated Nafion membranes

Model

To build a model of the hydrated Nafion membrane we used a Nafion monomer CF_3-$(CF_2)_{11}$-CF(CF_3)-O-CF_2-CF(CF_3)-O-CF_2-CF_2-SO_3^- with an equivalent weight of 1081 g/mol Nafion per sulfonate group. This coincides with the best studied membranes Nafion 117. The intramolecular interactions of Nafion and the intermolecular interactions Nafion - water have been described by the Dreiding force field [29]. For water we used our reactive force field in order to allow Grotthuss proton transfer within the framework of a classical MD simulation.

Table 1 The physical-chemical characteristics of the simulated water models

System	T [K]	P [MPa]	[g/sm^3]	[g/sm^3]	D_{exp} [$10^{-9}m^2/s$]	D_{sim} [$10^{-9}m^2/s$]
I	268	27	1.01	1.09	0.98	0.61
II	298	0.1	1.00	1.06	2.28	1.42
IV	298	210	1.07	1.12	2.27	1.31
III	423	10	0.92	0.93	12.9	9.97

Two system with different levels of hydration, λ=6 and λ=12, were considered (λ is the number of water molecules per sulfonate group of Nafion). To construct the systems of hydrated Nafion membrane with our reactive potential for water, we filled a cubic box with 36 Nafion monomers and added randomly the hydrogen and oxygen atoms accordingly to the hydration level (Table 2). It means that the initial systems contain free hydrogen and oxygen atoms and the ware molecules are formed during equilibration of the system. The selected procedure avoids any prejudgment in results.

The simulations of hydrated Nafion have been performed with DL_POLY2 at standard conditions. In the first step the systems have been equilibrated in NPT ensembles for 1.000.000 iterations with a time step of 0.2 *fs*. The equilibrated structures were used to perform a molecular dynamics simulation over 4.000.000 iterations in a NVT ensemble. The obtained trajectories were evaluated to determine the lifetime of hydronium ions and the Haven ratio. Both properties give valuable information about the mechanism of conductivity in the membrane.

Results of modeling for the hydrated Nafion membrane

Structure of the hydrated Nafion membranes

The equilibration of the Nafion membranes with the different hydration levels results in basically different morphologies. At low hydration level λ=6 (see Fig. 5) one can recognize isolated domains of water (red-white regions), surrounded by sulfonate groups (yellow-red) embedded in a Nafion matrix (blue-gray). In the hydrated Nafion membrane with high level of hydration λ=12 these domains are well percolated (Fig. 6). This is in a good agreement with the experimental results obtained by Gebel [30] and Capehart [31], where it was shown that only membranes with a hydration level λ>8 are fully penetrated by the aqueous domain.

Table 2 Characteristics of simulated systems

System	Particles	Number	Charge
λ=6	Nafion monomer	36	−.417 (on
	oxygen atoms		sulfonate group)
2988	hydrogen atoms	36×6=216	−.834
atoms			
box		216×2+36=468	+.417
34×34			
λ=12	Nafion monomer	36	−.417 (on
	oxygen atoms		sulfonate group)
3636			−.834
atoms			
box	hydrogen atoms	36×12=432	+.417
36×36		432×2+36=900	

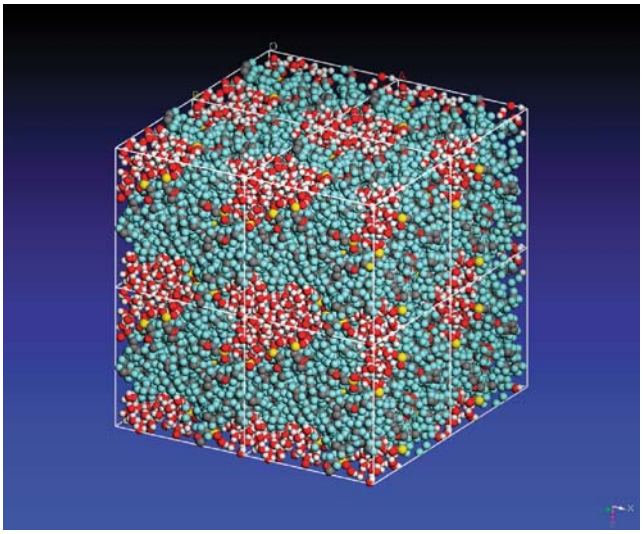

Fig. 5 Equilibrated structure of the Nafion membrane at low hydration level

In Fig. 7 we show the structure of water of a pore for the case of highly hydrated membrane λ=12. The Nafion backbone is omitted on this picture and only the water molecules and sulfonate groups of the polymer are plotted. One can recognize a network of water molecules, which are connected by pseudo-tetrahedrally coordinated hydrogen bonds. In this polar phase the hydronium ions are interspersed. We marked on this figure two hydronium ions. The first one takes place in the vicinity of the sulfonate groups of Nafion (white circle) and another is forming an Eigen ion (red circle). The third type of hydronium ions can be observed in Fig. 9b. There it forms the transition state during the proton transfer (Zundel ion).

A more detailed analysis of the water structure in the swollen membrane is given in Fig. 8. In this figure we differentiate between the two types of oxygen atoms: oxygen belonging to water molecule and oxygen making part of a hydronium ion. The distribution of hydrogen atoms around "water" oxygen (dashed lines) is very similar to the experimental RDF's for bulk water in Fig. 2.

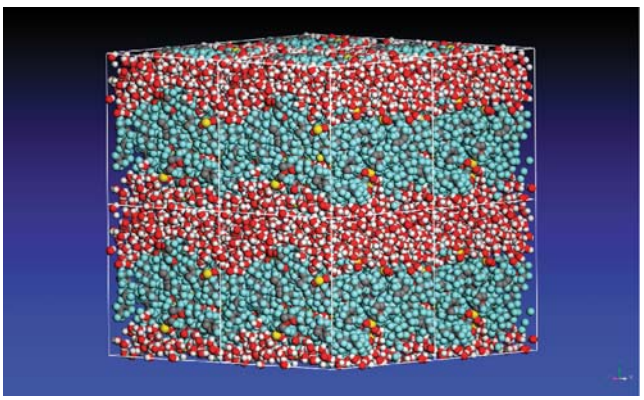

Fig. 6 Equilibrated structure of the Nafion membrane at high hydration level

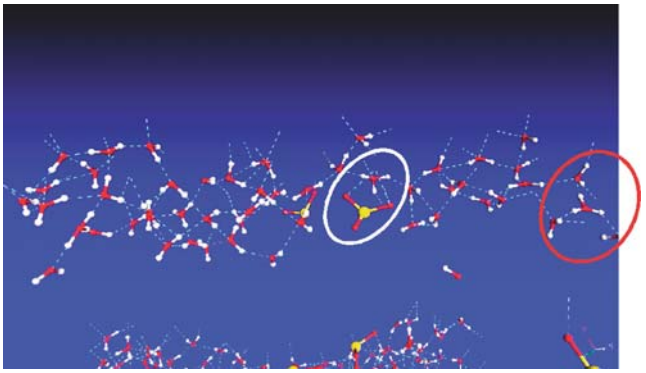

Fig. 7 The structure of water in one pore of the highly hydrated Nafion membrane

However, the peaks have different height as a consequence of the confinement inside the matrix of Nafion. The RDF's of the "hydronium" oxygen differs from the "water" oxygen mainly by the peak around 2Å. This peak nearly disappears indicating that the hydronium ions are not coordinated by further hydrogen bonds as we discussed in the chapter "Structural properties". The picture is very similar to the recent first principle studies of hydronium ion in water [32].

Proton transfer

Firstly we investigated the question if the new force field allows bond breaking/formation. This feature is the basic requirement to describe the Grotthuss mechanism. The importance of the Grotthuss mechanism for the conductivity in membranes is broadly accepted.

To trace a proton transfer we prepared a movie, where we follow one hydronium ion inside the membrane. The full film can be found in the Electronic Supplementary Material to this article. In Fig. 9 we show three snapshots from this movie. The atoms of the Nafion matrix are shown in a big ball, water molecules inside the membrane in small balls, and the particles of interest, hydronium ion and water molecule, are marked by medium size balls. On the first snapshot the hydronium ion and water molecule are

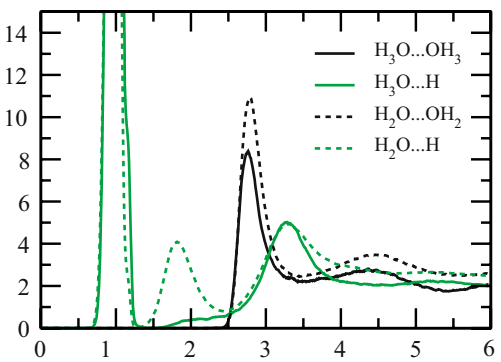

Fig. 8 The coordination of water molecules and hydronium ions in the Nafion membrane (λ=12)

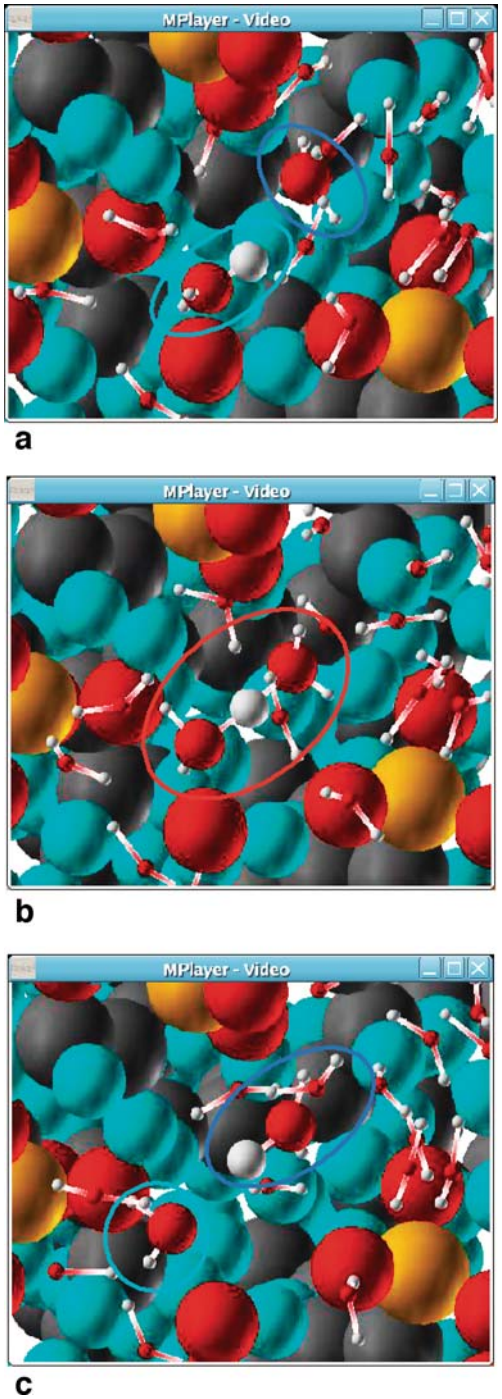

Fig. 9 Proton transfer inside a swollen Nafion membrane. (**a**) In the beginning of our simulation we marked one hydronium ion (violet) and one water molecule (blue). (**b**) After some *ps* a Zundel ion (red) is formed. (**c**) Finally a proton transfer occurs and the new formed water molecule (violet) and hydronium ion (blue) separates

separated. On the middle snapshot these two species come closer and form a transition complex (Zundel ion). The last snapshot illustrates the situation after proton hopping.

Visually the process of proton transfer includes two steps. In the first, slow step, two species, hydronium ion and water molecule, move closer to get preferable orientation to build an intermediate complex (Zundel ion). In the second step, quick one, the proton vibrates between the two oxygen atoms of this complex. Finally, the Zundel ion breaks and the excess hydrogen atom bonds randomly to one of the two water molecules. In the illustrated case it was transferred, but nearly with the same probability it can turn back to the original water molecule. Afterwards the newly formed hydronium ion continues the movement to meet the next water molecule.

Lifetime of hydronium

Important information about the mechanism of proton transfer in the membrane can be obtained by a detailed analysis of the lifetime of hydronium ions. To calculate lifetimes we introduced the hydronium specification function, $h(H_30^+)$. This function assigns to each oxygen atom *1*, if it has three bonds, and *0* to the all other oxygen atoms. The initial number of hydronium ions should be 36 assuming full dissociation for all sulfonate groups. For the low hydrated Nafion membrane the initial value of hydronium ions is equal to 36, which exactly coincides with the expected value. For the high hydrated system the initial value of hydronium ions is equal to 42, which is caused by a small additional auto-dissociation of water.

The normalized, time dependent autocorrelation of the hydronium specification function $h(\mathrm{H_30^+})$ is plotted in Fig. 10.

$$n(H_3O^+) = \left\langle h\left(\overrightarrow{0}\right) h\left(\overrightarrow{t}\right) \right\rangle \tag{7}$$

From these data one can derive the reaction order of the hydronium decay, following the procedure described in standard textbooks [33]. For this purpose the number of hydronium ions is plotted in different scales versus the time. For the first order, the presentation of the logarithm, for the second order, the inverse, and for the third order, the inverse in the square should correlate linear in time. Figure 11 displays the result. The integrated rate law of second order is perfectly fulfilled and the time is linear to the inverse of the hydronium ions $n_{H_30^+}(t)$.

$$t \propto {}^{1}/_{n_{H_3O^+}} \tag{8}$$

This implies that two particles are participating in the time-determining reaction. This result coincides with the impression gained from the movie. Inside the membranes, at least at low water content, the time determinant step for the proton transfer is the diffusion of the hydronium ion and one water molecule to form a precursor complex. In a second step the proton transfer takes place. However, this step is so quick, that it does not influence significantly the kinetics of proton transfer in membrane. Recent first principle molecular dynamic studies confirm the very quick

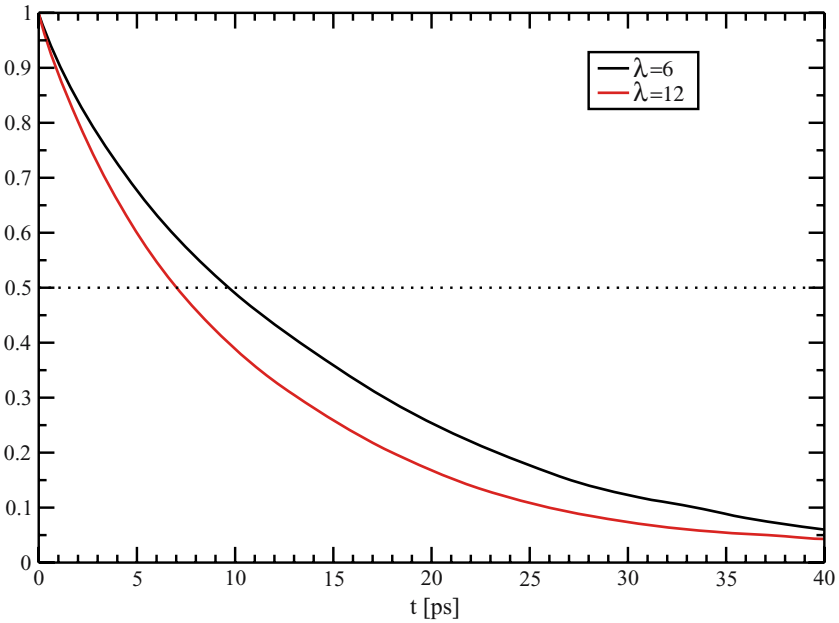

Fig. 10 Autocorrelation function of the hydronium $n_{H_3O^+}$ specification function

proton transfer and calculate the transition time as quick as 140 *fs* [32].

Another indication to a second order reaction for the proton transfer is given by the dependence of hydroniums lifetime from water content following from Fig. 10. The lifetime of hydronium ions is shorter at higher content of water, where the hydronium ion needs less time to meet water molecule with preferable orientation for building the precursor complex.

A similar case has been recently studied experimentally. The relaxation of the bond stretching in HOD also depends in the Nafion membranes on the water content [34]. The slow step in this reaction might be the diffusion of the excited water to meet a second water molecule. Then they form a precursor complex to perform finally the quenching of the excitation.

In both cases mentioned above the reactions becomes of first order for pure water. At very high concentrations of water the reactions obey a law of pseudo-first order [35]. The forming of the precursor complex becomes very fast and the kinetics of proton transfer is determined by the second step.

Diffusion, conductivity and Haven ratio

It is well known that the collective correlations between protons/hydrogens increase strongly the proton conductivity in the membranes, as it is evidenced by the deviation

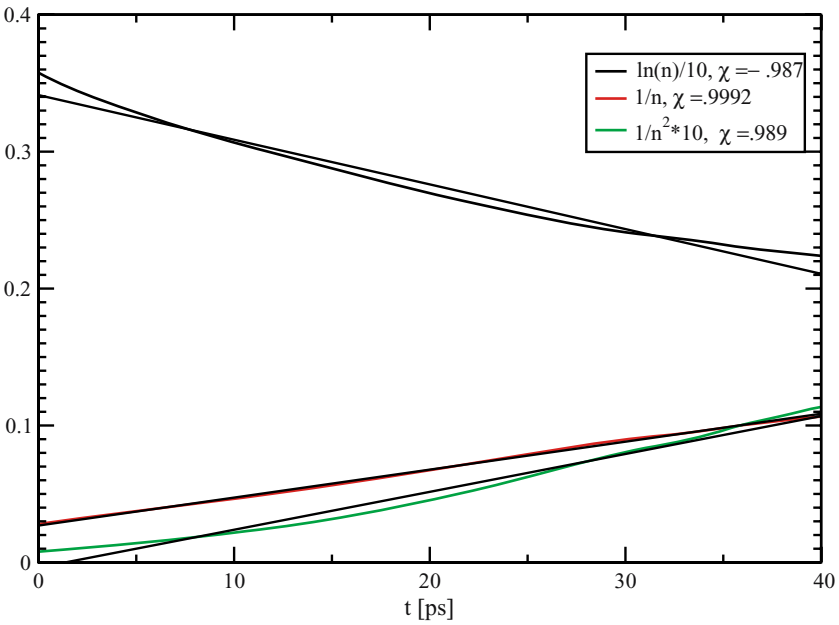

Fig. 11 Analysis of the reaction order. Second order (red) gives perfect agreement

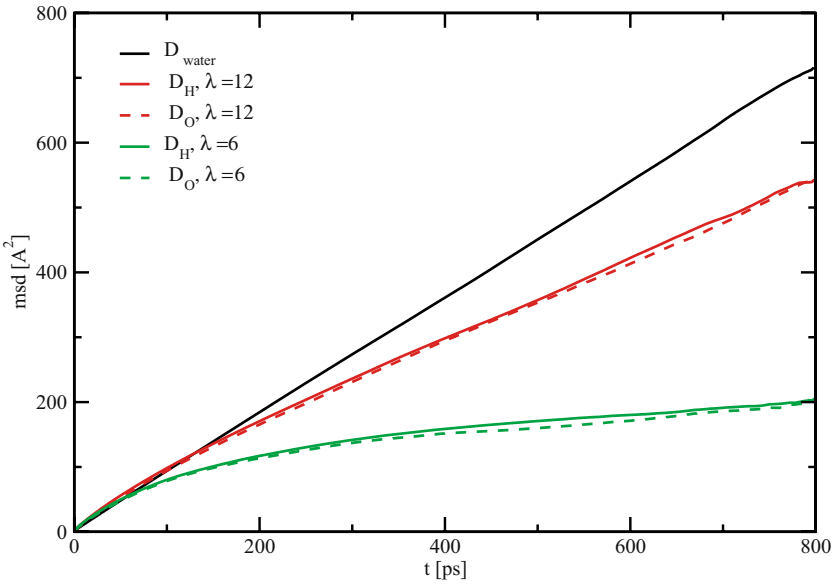

Fig. 12 Mean square displacements of hydrogen and oxygen atoms in the Nafion membrane

from the Nernst-Einstein equation. The conductivity σ has to be related with the diffusion coefficient D_{H^+} by proportional factor $\frac{n_{H^+}q_{H^+}}{k_BT}$ in accordance to the modified Nernst-Einstein equation.

$$\sigma = \frac{1}{H_R}\frac{n_{H^+}q_{H^+}}{k_BT}D_{H^+} \tag{9}$$

In this formula n_{H^+} is the formal number of protons in the system (in our case 36) and q_{H^+} is a formal charge of $+1e$. The Haven ratio H_R is a collective correlation factor. For completely independent charge carriers the Haven ration becomes one ($H_R = 1$) and the traditional Nernst-Einstein equation is recovered. For high concentrated salt solutions the value of H_R is above one. It expresses the tendency of ions with opposite charges to migrate together diminishing the total conductivity. For ion conducting polymers, when only the cations are allowed to move and the anions are fixed, simple models [36] predict a Haven ratio below one ($H_R < 1$).

To calculate the correlation factor (i.e., value of Haven ratio H_R) for the case of the hydrated Nafion membranes, the self-diffusion coefficients D_{H^+} and the conductivity σ are needed.

The required self-diffusion coefficients D_{H^+} can be estimated relatively easily from MD simulations. The diffusion coefficient D_{H^+} is accessible by the Einstein relation:

$$D = \lim_{t\to\infty}\frac{1}{6t}\left\langle\left[R_i\left(\vec{t}\right) - R_i\left(\vec{0}\right)\right]^2\right\rangle = \lim_{t\to\infty}\frac{1}{6t}msd \tag{10}$$

In Fig. 12 the mean square displacement (*msd*) of the hydrogen and oxygen atoms are plotted. For comparison, the *msd* for pure water are added to this graph (black). One can see that for short calculation times the self-diffusion coefficients for both hydration levels of Nafion are similar to the self-diffusion of pure water. In the low hydrated membrane the confinement of the water by the surrounding Nafion matrix becomes recognizable after 50 *ps* (green curve) and the curve lowers the slope. For the high hydrated membrane the diffusion is influenced by the confinement after 100 *ps* (red curve). The last fact reflects the morphologic difference in membranes with different level of hydration. The absolute values for the diffusion coefficients are obtained from the slope of the plotted curves. For the low hydrated membrane the simulated diffusion coefficient of $3.2*10^{-6}$ cm^2/s is slightly below the experiment, $3.7*10^{-6}$ cm^2/s [37]. For the high hydrated

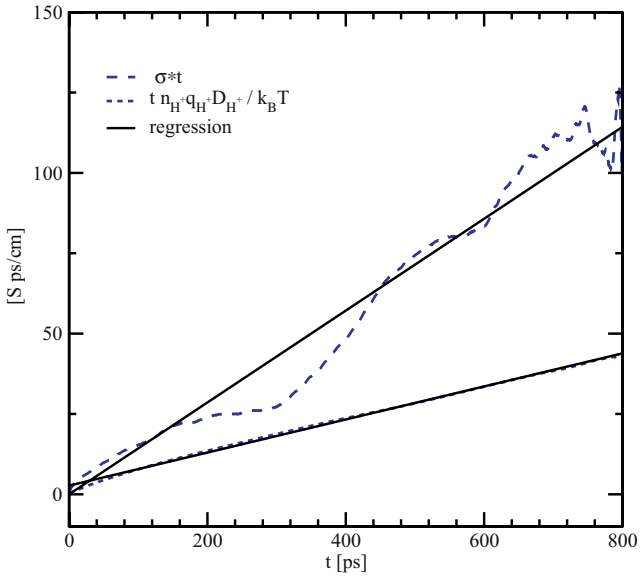

Fig. 13 Conductivity of the high hydrated membrane estimated from diffusion and Einstein equation

membrane the diffusion coefficient of $10.5*10^{-6}$ cm^2/s is above the experimental value of $5.2*10^{-6}$ cm^2/s. The reason might be the difference in the tortuosity of the simulated and the real membrane, e.g., some pores in the real membrane have dead ends.

Equation 9 needs in addition the conductivity σ to determine the Haven ratio H_R. The conductivity can be calculated by the Einstein equation from trajectories:

$$\sigma = \frac{F^6}{RT6t}\left\langle \left\{ \sum_i z_i [R_i(t) - R_i(0)] \right\}^2 \right\rangle \tag{11}$$

Unfortunately, for the low hydrated membrane the correct estimation of conductivity was not possible by reasons of scarce statistics: the error for the derived conductivity has the same magnitude as the value of conductivity itself. For the high hydrated membrane the simulated conductivity overshoots the experimental value, 0.14 S/cm versus 0.05 S/cm [1].

This result is analogous to the results obtained for self−diffusion coefficients. The guessed reason is the lower tortuosity of the simulated system compared with the real membrane. The effect of tortuosity can be assumed for diffusion and conductivity to be very similar. A pore with dead end neither contributes to diffusion nor to the conductivity. Therefore, the ratio of both values should not be affected by the error of the incorrect tortuosity.

For the simulated Nafion membrane with $\lambda=12$ we obtained for the Haven ratio 0.33, which is in satisfactory agreement with experimental value of 0.46 given in [1]. According to these results we can estimate the contribution of the diffusion mechanism to total conductivity of membrane as one third. The other two third are caused by a collective movement of hydrogen atoms and protons.

In Fig. 13 we give the total conductivity σ and the diffusion coefficient σ_D multiplied with the proportional factors. It clearly follows from this figure that the total conductivity is significantly higher than the diffusion based conductivity.

Following the discussion above a future improving of membranes can be the control of the collective moving of protons and hydrogen atoms in the system: with the increasing of the collective moving, the Haven ratio decreases significantly and causes the increasing of conductivity in accordance with Nernst-Einstein Eq. 9. In other systems, dried NaOH, the conductivity exceeds the proton diffusion by four magnitudes [38].

Conclusions

The new reactive force field reproduces the experimental radial distribution functions of water very accurately as a consequence of the recursive fitting. Within our reactive water model the main structural features of bulk water as well as water inside Nafion membrane can be fulfilled. The reactive force field allows bond-breaking/formation on a classical level and is simple enough to simulate such complicated systems as polyelectrolyte Nafion membranes. It is found that the proton transfer in low hydrated membranes is a second order reaction, which is mainly determined by the formation of a precursor complex. In a second, quick reaction the proton transfer occurs. The conductivity of membrane is strongly determined by a collective movement of protons and hydrogen's, which increases the conductivity far beyond a simple diffusion mechanism.

Acknowledgments The authors would like to thank for financial support the Sardinia Region and the Italian Ministry of Research (MIUR), NUME project (http://www.progetto-nume.it/). The authors are also indebted to Lorenzo Pisani for many useful discussions.

References

1. Kreuer KD, Paddison SJ, Spohr E, Schuster M (2004) Chem Rev 104:4637–4678
2. Tuckerman M, Laasonen K, Sprik M, Parrinello MJ (1995) Chem Phys 103:150–161
3. Schmitt U, Voth G (1999) J Chem Phys 111:9361–9381
4. Walbran S, Kornyshev A (2001) J Chem Phys 114:10039–10048
5. Day T, Soudackov A, Cuma M, Schmitt U, Voth G (2002) J Chem Phys 117:5839–5849
6. Spohr E, Commer P, Kornyshev A (2002) J Phys Chem B106:10560–10569
7. Petersen M, Wang F, Blake N, Metiu H, Voth G (2005) J Phys Chem B 109:3727–3730
8. van Duin A, Dasgupta S, Lorant F, Goddard III W (2001) J Phys Chem A 105:9396–9409
9. Yin K, Xia Q, Xu D, Chen C (2006) Comput Chem Eng 30:1346–1353
10. Lyubartsev A, Laaksonen A (2000) Chem Phys Lett 325:15–21
11. Wernet P, Nordlund D, Bergmann U, Cavalleri M, Odelius M, Ogasawara H, Naslund LA, Hirsch TK, Ojamae L, Glatzel P et al. (2004) Science 304:995
12. Soper AK (2000) Chem Phys 258:121–137
13. Hofmann D, Apostolakis J (2003) J Mol Struc:Theo Chem 647:17–39
14. Lemberg H, Stillinger FH (1975) J Chem Phys 62:1677–1690
15. Arthur J, Haymet ADJ (1998) Fluid Phase Equilibria 150:91–96
16. Bresme F (2001) J Chem Phys 115:7564–7574
17. Soper AK (1996) Chem Phys 202:295–306
18. Lyubartsev A, Laaksonen A (1995) Phys Rev E52:3730–3737
19. Bernal J, Fowler RH (1933) J Chem Phys 1:515–548
20. Elliot J, Hanna S, Elliot A, Cooley G (1999) Phys Chem Chem Phys 1:4855–4863
21. Hofmann D, Kuleshova L, D'Aguano B (2007) Phys Chem Let 448:138–143
22. Matsuoka O, Clementi E, Yoshimine M (1976) J Chem Phys 64:1351–1361
23. Bursulaya B, Kim H (1998) J Chem Phys 109:4911–4919

24. Guillot B (2002) J Mol Liquids 101:219–260
25. Watanabe K, Klein M (1989) Chem Phys 131:157–167
26. Berendsen H, Postma J, van Gunsteren W, Hermans J (1981) Interaction models for water in relation to protein hydration. In: Pullmann, Dodrecht (eds) pp 331–342
27. Wallqvist A, Astrand P-O (1995) J Chem Phys 102:6559–6565
28. Silvestrelli P, Parrinello M (1999) J Chem Phys 111:3572–3580
29. Mayo SL, Olafson BD, Goddard III WA (1990) J Phys Chem 94:8897–8909
30. Gebel G (2000) Polymer 41:5829–5838
31. Wescott J, Qi Y, Subramanian L, Capehart T (2006) J Chem Phys 124:134702–134716
32. Boero M, Ikeshoji T, Terakura K (2005) Chem Phys Chem 6: 1775–1779
33. Wedler G (1982) Lehrbuch der physikalischen Chemie. In Verlag Chemie; Chapter Die Bestimmung der Reaktionsordnung, pp 161–165
34. Moilanen DE, Piletic IR, Fayer MD (2006) J Phys Chem A110:9084–9088
35. Lowry TH, Richardson KS (1981) Mechanism and theory in organic chemistry. In: second ed.; Haper & Row, Publishers:; Chapter Kinetics and Mechanism, pp 174–188
36. Lonegran M, Shriver D, Ratner M (1995) Electrochimica Acta 40:2041–2048
37. Zawodzinski T, Derouin C, Radzinski S, Sherman R, Smith V, Springer, T, Gottesfeld A (1993) J Electrochem Soc 140:1041–1047
38. Spaeth M, Kreuer K, Maier J, Cramer C (1999) J Solid State Chem 148:169–177